

Study of fermion pair events at the 250 GeV ILC

Yuto Deguchi^{*1}, Hiroaki Yamashiro¹, Taikan Suehara¹, Tamaki Yoshioka²,
Keisuke Fujii³, and Kiyotomo Kawagoe¹

¹Department of Physics, Faculty of Science, Kyushu University, Fukuoka, Japan

²Research Center for Advanced Particle Physics, Kyushu University, Fukuoka, Japan

³High Energy Accelerator Research Organization (KEK), Tsukuba, Japan

Abstract

Precise measurements of electroweak processes at the International Linear Collider (ILC) will provide unique opportunities to explore new physics beyond the standard model. Fermion pair production events are sensitive to new interactions involving a new heavy gauge boson or an electroweak interacting massive particle (EWIMP). We studied the mass reach of new particles at the ILC with $\sqrt{s} = 250$ GeV by using $e^+e^- \rightarrow e^+e^-$ and $e^+e^- \rightarrow \mu^+\mu^-$ events. We obtained the new mass reaches BSM particles with 90% confidence level using a toy Monte Carlo technique.

1 Introduction

The International Linear Collider (ILC)[1] is an electron-positron linear collider, which is planned to be constructed in Japan. The main purposes of the ILC are discoveries of new particles and precise measurement of the Higgs boson and the top quark. The center of mass energy will be 250 GeV with 20 km tunnel length. In the future, the center of mass energy can be upgraded to 1 TeV with 50 km tunnel length.

We know that the reaction of $e^+e^- \rightarrow 2f$ events involve the emission and absorption or exchange of Z bosons in the Standard Model. In some models beyond the Standard Model (BSM), additional particles can also contribute to the interaction. Precise measurements of electroweak processes at the ILC can search these particles.

In this paper, We studied effects of new heavy gauge bosons (Z' particles) with five BSM models and electroweak WIMPs with three BSM models. We calculated the mass reach of new particles at the ILC with $\sqrt{s} = 250$ GeV by using $e^+e^- \rightarrow e^+e^-$ and $e^+e^- \rightarrow \mu^+\mu^-$ events. We observed the effect of BSM models on the cross section of the final state leptons and the angular distributions. We calculated the mass limit of each model with toy Monte Carlo technique to make pseudo experiments.

2 Models

In this study, we considered five types of Z' , which are Sequential Standard Model (SSM), E_6 group (χ model, ψ model, η model), and Alternative Left-Right symmetry (ALR)[2]. These Z' bosons are exchanged between leptons, like Z boson, when electroweak interactions occur (See Fig.1).

^{*}Presenter. Talk presented at the International Workshop on Future Linear Collider (LCWS2018), Arlington, Texas, 22-26 October 2018. C18-10-22.

34 We also considered three EWIMP models, which are Minimal Dark Matter (MDM), Higgsino, and
 35 Wino[3]. These particles couple to the Z' boson in a loop contribution (See Fig.2), which affects the
 $e^+e^- \rightarrow 2f$ interaction. The quantum numbers of each EWIMP models are shown in Table 1.

Table 1: Quantum numbers of each model

model	$SU(2)_L$	$U(1)_\gamma$ hypercharge
MDM	$n = 5$ (pentet)	0
Higgsino	$n = 2$ (doublet)	$\pm 1/2$
Wino	$n = 3$ (triplet)	0

36

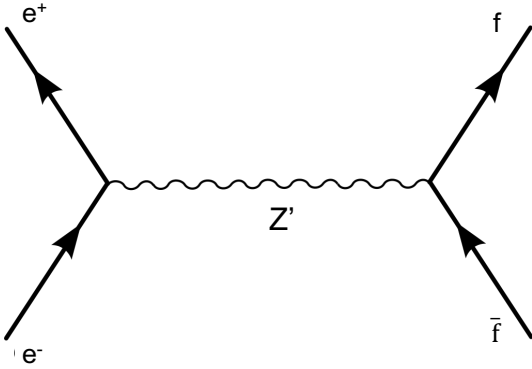


Figure 1: Feynman diagram involving Z'

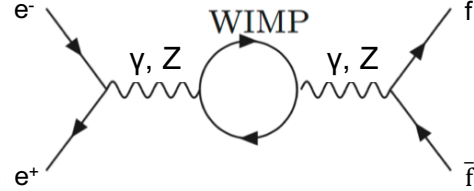


Figure 2: Feynman diagram involving EWIMP

37 3 Simulation

38 In this study, we used the ILCsoft[4] v01-16-p10 for the simulation and reconstruction. We used samples
 39 prepared for Detailed Baseline Design (DBD) of International Large Detector (ILD)[5] concept. The
 40 samples were generated by WHIZARD 1.95[6], and simulated by Mokka, with detector geometry
 41 of ILD_v1_o5. There is a special treatment of $e^+e^- \rightarrow e^+e^-$ samples, which includes preselection
 42 of xxxxxx. It was also prepared with weighted production, which produces the same amount of
 43 events for each $\cos\theta$ bins of 0.1 width. The ILD detector consists of vertex detector, a tracking
 44 detector, an electromagnetic calorimeter, and a hadron calorimeter. These detectors are located inside
 45 a superconducting solenoid with 3.5 Tesla magnetic field. The magnetic flux of the coil is returned
 46 in an iron yoke, equipped with a muon detector. The center of mass energy is $\sqrt{s} = 250$ GeV and
 47 the total luminosity is 2000 fb^{-1} . The beam polarization was set to 80% left-handed for the electron
 48 beam and 30% right-handed for the positron beam. The luminosity of left-handed electron and right-
 49 handed positron is 900 fb^{-1} , and right-handed electron and left-handed positron is also 900 fb^{-1} .
 50 After the detector simulation, the events are reconstructed by Marlin[7], including Pandora PFA[8] for
 51 track-cluster matching.

52 4 Event selection

53 In this section, we explain the separation of background events from signal events.

54 4.1 $e^+e^- \rightarrow e^+e^-$

55 To select the $e^+e^- \rightarrow e^+e^-$ events, we considered five cut terms. The final states of background events
 56 are $e^+e^- \rightarrow \mu^+\mu^-$, $e^+e^- \rightarrow \tau^+\tau^-$, and $e^+e^- \rightarrow 4f$ events, with only lepton in the final states. Firstly,
 57 we selected tracks with energy $E_{tr} > 15$ GeV. Events which do not have positive and negative tracks
 58 meeting the requirement are removed. If there are more than one pair of such tracks, the track of
 59 highest energies are selected for both positive and negative charge. After that, we applied following
 60 selection conditions.

- 61 • The ratio of energy deposit at calorimeter to the energy of track : $E_{cal}/E_{tr} > 0.8$ to reject muon
 62 events.
- 63 • $E_{ecal}/(E_{ecal} + E_{hcal}) > 0.85$ to separate hadrons and muons. E_{ecal} is the energy deposit at the
 64 electromagnetic calorimeter, and E_{hcal} is the energy deposit at the hadron calorimeter.
- 65 • The energy sum of two tracks : $E_{sum} > 230$ GeV to exclude 4 fermion events and tau events.
- 66 • $|\cos\theta| < 0.95$ to cut t-channel $e^+e^- \rightarrow e^+e^-$ events which have huge cross section at the forward
 67 angle. θ is the angle of the track with respect to the beam axis.

68 The result of event selection is shown in Table 2. Most of background events can be excluded by
 these cut terms.

Table 2: Event selection of electron channel

Cut terms	signal(e^+e^-)	$\mu^+\mu^-$	$\tau^+\tau^-$	$4f$
all events	8.26×10^8	9.73×10^6	1.17×10^7	7.73×10^6
$E_{tr} > 15$ GeV	8.18×10^8	9.36×10^6	1.17×10^7	6.39×10^6
$E_{cal}/E_{tr} > 0.8$	8.18×10^8	2.91×10^4	1.17×10^7	2.60×10^6
$E_{ecal}/(E_{ecal} + E_{hcal}) > 0.85$	8.17×10^8	1.22×10^4	1.17×10^7	1.66×10^6
$E_{sum} > 230$ GeV	3.68×10^8	14	21	1.14×10^4
$ \cos\theta < 0.95$	2.57×10^7	14	21	1.14×10^4

69

70 4.2 $e^+e^- \rightarrow \mu^+\mu^-$

71 We selected most energetic tracks of positive and negative charge with $E_{tr} > 15$ GeV as same as
 72 $e^+e^- \rightarrow e^+e^-$ case, then we applied following selection conditions.

- 73 • $E_{cal}/E_{tr} < 0.3$ and $E_{ecal}/(E_{ecal} + E_{hcal}) < 0.45$ to reject electrons and hadrons.
- 74 • $E_{sum} > 230$ GeV to exclude 4 fermion and tau events.
- 75 • $|\cos\theta| < 0.95$ to cut t-channel $e^+e^- \rightarrow e^+e^-$ events.

76 The result of event selection is shown in Table 3. We could also exclude most of background events.

77 5 Analysis

78 After the event selection, we obtained the angular distribution for each channel with 20 bins, shown
 79 in Fig.3 and Fig.4. Vertical axis of the electron channel is logarithmic scale, and vertical axis of the
 80 muon channel is linear scale. The mass reach of new particle were calculated using these angular
 81 distributions.

Table 3: Event selection of muon channel

Cut terms	signal($\mu^+ u^-$)	e^+e^-	$\tau^+\tau^-$	$4f$
all events	9.73×10^6	8.26×10^8	1.17×10^7	7.73×10^6
$E_{\text{tr}} > 15 \text{ GeV}$	9.36×10^6	8.18×10^8	1.17×10^7	6.39×10^6
$E_{\text{cal}}/E_{\text{tr}} < 0.3$	9.26×10^6	1.49×10^6	8.97×10^5	3.35×10^6
$E_{\text{ecal}}/(E_{\text{ecal}} + E_{\text{hcal}}) < 0.45$	2.91×10^6	1.49×10^6	7.80×10^5	1.33×10^6
$E_{\text{sum}} > 230 \text{ GeV}$	7.49×10^5	56	4.52×10^3	32
$ \cos\theta < 0.95$	7.48×10^5	56	4.48×10^3	32

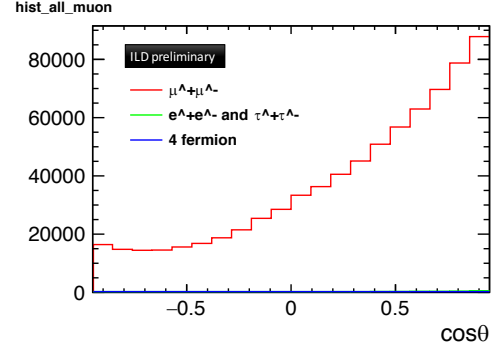
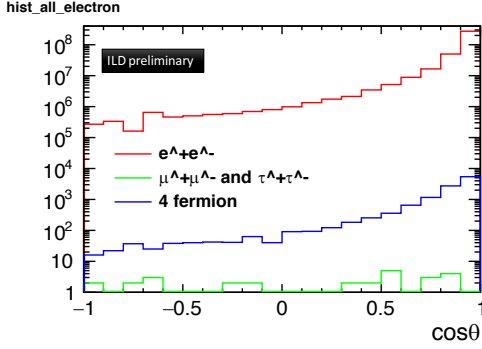


Figure 3: Angular distribution of electron channel

Figure 4: Angular distribution of muon channel

82 First, we calculated deviations of particle cross section with each BSM model at each bin. Second,
 83 we made pseudo experiments for each bin using SM angular distribution with fluctuation of the Poisson
 84 distribution. Third, we calculated χ^2 between the pseudo experiments and the each BSM model
 85 to obtain probability. At this time, 0.1% systematics are assumed for each bin. The distributions
 86 of probability are shown in Fig.5 and Fig.6. Finally, We obtained medians from the probability
 87 distributions of each BSM model. Mass dependence of the probability for each particles is shown in
 88 Fig.7 and Fig.9. The blue lines where the probability is 0.1 show 90% confidence level mass limit.
 89 These values for each particle are shown in Table 4 and Table 5.

Table 4: Mass reach of Z'

BSM	mass reach (90% CL)
SSM	3.4 TeV
ALR	5.0 TeV
χ	3.5 TeV
ψ	1.7 TeV
η	1.7 TeV

Table 5: Mass reach of EWIMP

BSM	mass reach (90% CL)
MDM	500 GeV
Higgsino	180 GeV
Wino	240 GeV

90 The mass reaches of Z' are comparable to LHC. Thus we have to conclude that the CM energy
 91 should be much higher than 250 GeV to obtain significant gain of measurement from LHC results.
 92 The mass reaches of EWIMP are bigger than 125 GeV, which is the limited direct search, so we think
 93 the $e^+e^- \rightarrow 2f$ can be a powerful prove to look for such a new physics.

6 Summary

We are investigating the effects from BSM models on $e^+e^- \rightarrow 2f$ final states at e^+e^- colliders. We obtained the mass reach of the new BSM particles at 90% confidence level at ILC with $\sqrt{s} = 250$ GeV. In this paper, we considered the mass reach using $e^+e^- \rightarrow e^+e^-$ and $e^+e^- \rightarrow \mu^+\mu^-$, but we didn't include $e^+e^- \rightarrow \tau^+\tau^-$. We expect that better mass reach can be obtained by including tau and hadron channel.

Acknowledgements

We thank ILD physics and software group for generating events and many support, and we thank Dr. Satoshi Shirai for providing the cross sections with EWIMP models. This work was supported by JSPS KAKENHI Grant Number 16H02176.

References

- [1] Ties Behnke et al., The International Linear Collider Technical Design Report - Volume 1: Executive Summary, arXiv:1306.6327 (2013).
- [2] Paul Langacker. The physics of heavy Z' bosons. *Rev. Mod. Phys.*, 81:1199-1228 (2009).
- [3] Keisuke Harigaya, Koji Ichikawa, Anirban Kundu, Shigeki Matsumoto, and Satoshi Shirai, Indirect probe of electroweak-interacting particles at future lepton colliders, JHEP 1509 (2015).
- [4] <http://ilcsoft.desy.de/portal/>
- [5] Halina Abramowicz et al., The International Linear Collider Technical Design Report - Volume 4: Detectors, arXiv:1306.6329 (2013).
- [6] Wolfgang Kilian, Thorsten Ohi, and Jürgen Reuter. Whizard-Simulating Multi-Particle Processes at LHC and ILC. *Eur. Phys. J. C* **71** 1742 (2011).
- [7] http://ilcsoft.desy.de/portal/software_packages/marlin/
- [8] M. A. Thomson, Particle flow calorimetry at the ILC, AIP Conf. Proc. **896**, 215 (2007).

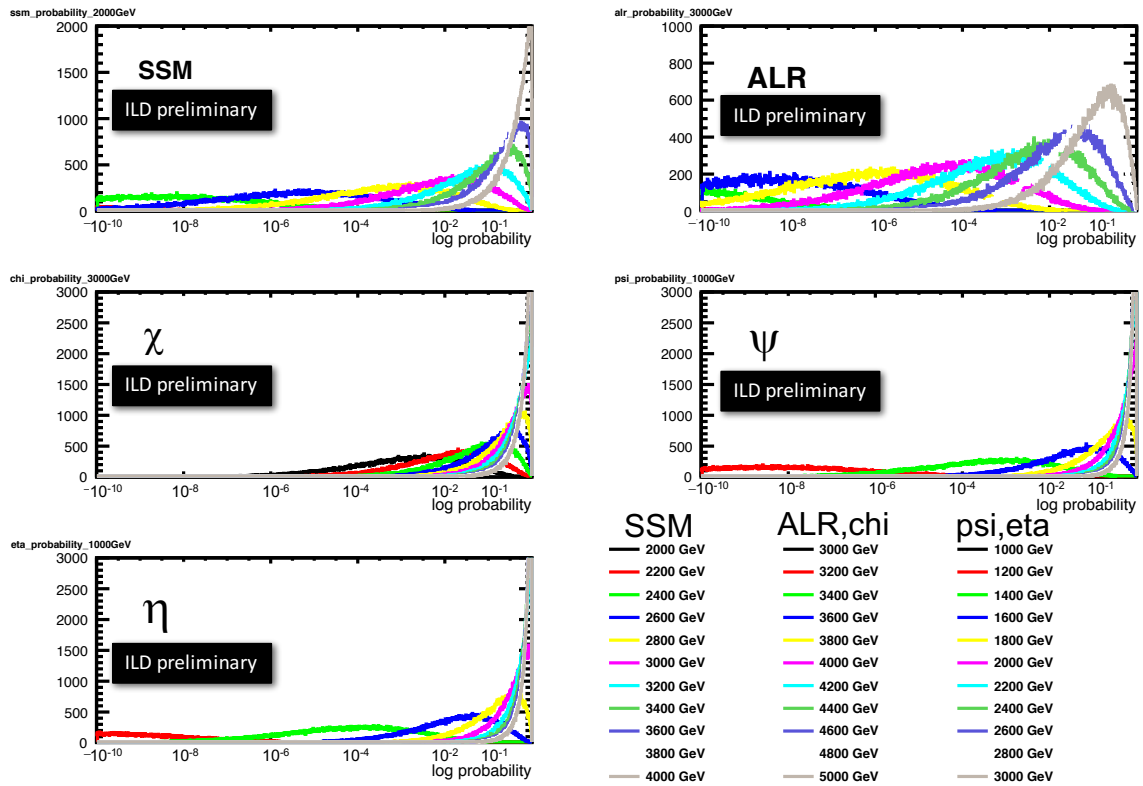


Figure 5: Probability distribution of Z' models with 100,000 pseudo experiments. The colors show different masses of Z' bosons as shown in the legend.

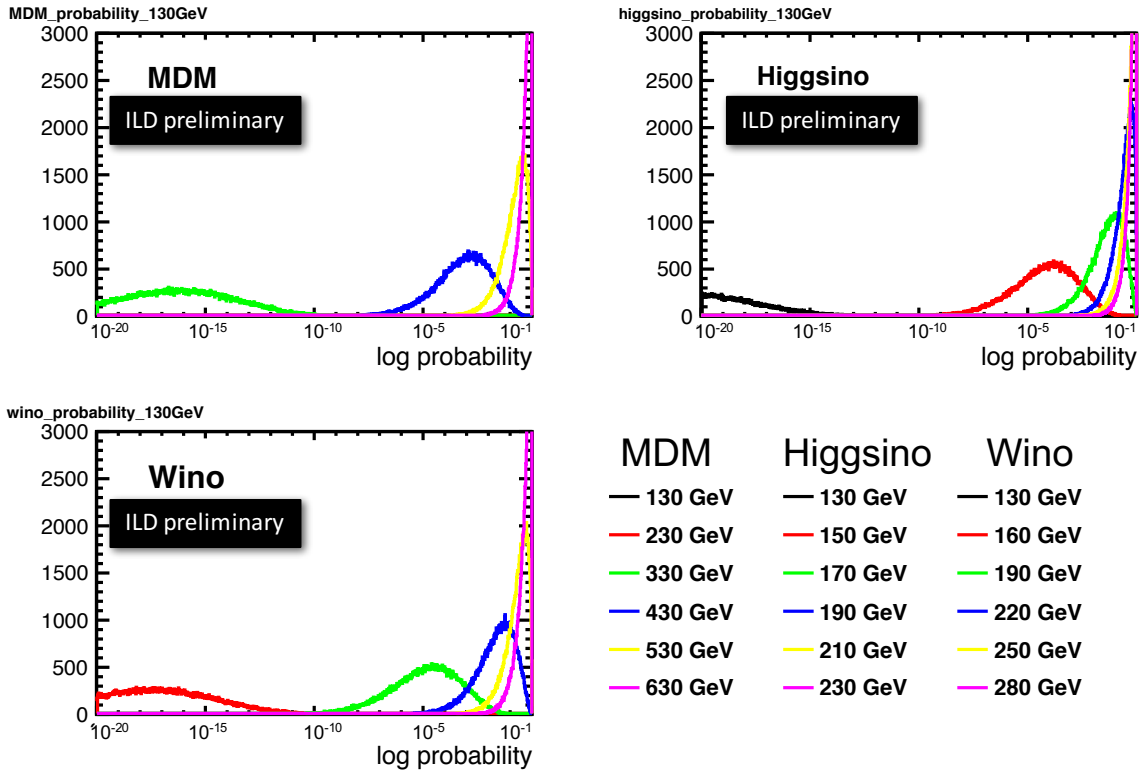


Figure 6: Probability distribution of EWIMP models with 100,000 pseudo experiments. The colors show different masses of EWIMPs as shown in the legend.

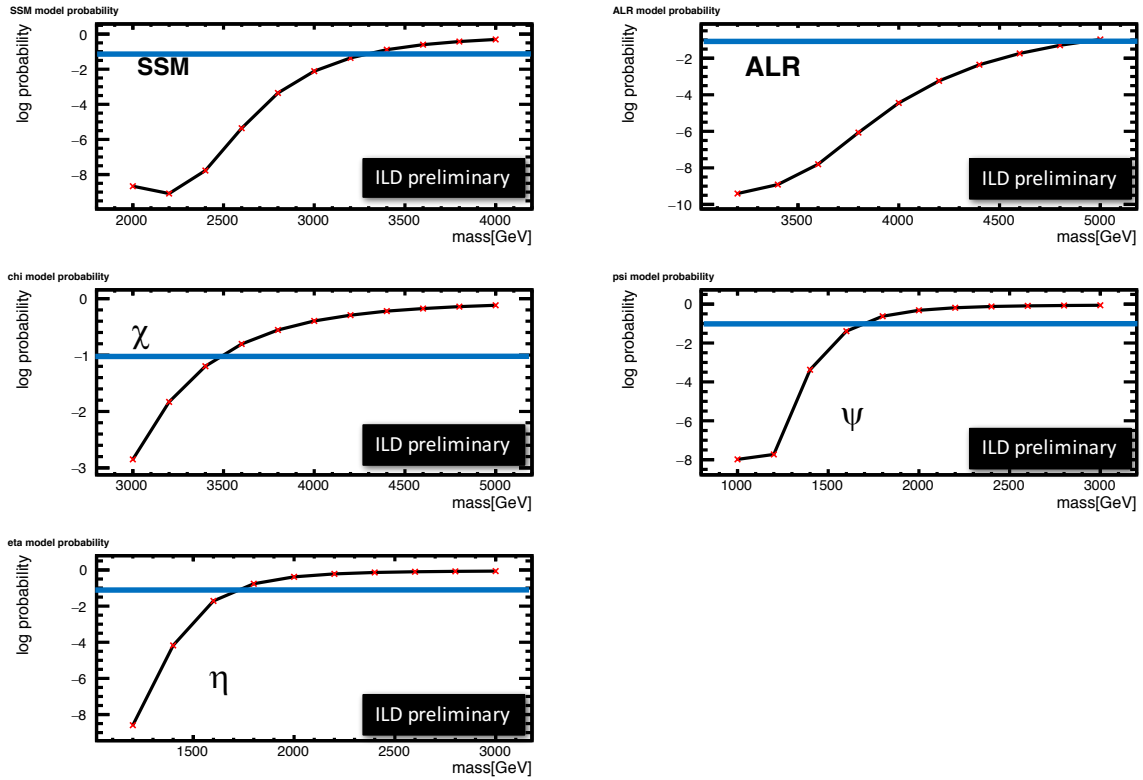


Figure 7: Median of the probability distribution obtained by pseudo experiments with Z' models. The blue lines show exclusion limit at 90% confidence level.

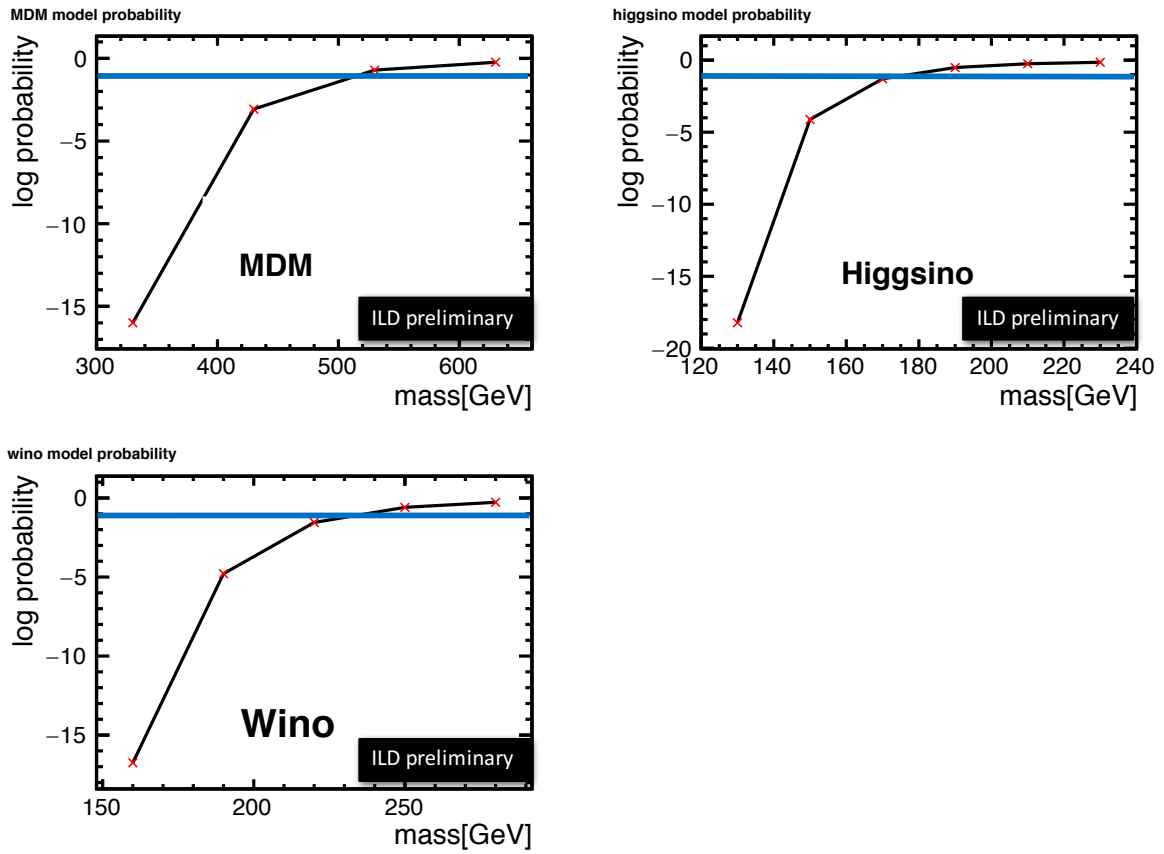


Figure 8: Median of the probability distribution obtained by pseudo experiments with EWIMP models. The blue lines show exclusion limit at 90% confidence level.